

AlN Contour Mode Resonators with Half Circle Shaped Reflectors

Zhifang Luo^{1,2,3,*}, Shuai Shao^{1,2,3}, Tao Wu^{1,*}

Abstract— AlN contour mode resonators (CMRs) with half circle shaped reflectors are designed to reduce the anchor loss. In this work, we use finite element analysis (FEA) and demonstrate that the half circle shaped reflector can effectively reduce the energy dissipation through the anchor to the plate, and then boost the CMR quality factor Q. Furthermore, the measured experimental data of AlN CMR with half circle shaped reflectors design yields a Q of 1605 operating at the resonance of around 400 MHz, which provides over 80% improvement compared to an AlN CMR with a normal plate configuration.

I. INTRODUCTION

Piezoelectric microelectromechanical resonators have shown many advantages in radio frequency (RF) filters, and miniature transducers [1–4]. Among various piezoelectric materials, such as Zinc Oxide (ZnO), piezoelectric ceramics (PZT), Lithium Niobate (LN) and Aluminum Nitride (AlN) [5–10], AlN-based resonators play a more important role in 5G communication, due to the high phase velocity of the AlN thin film and compatibility with CMOS process [9, 11, 12]. In the last decades, film bulk acoustic resonators (FBAR), surface acoustic wave (SAW) and contour mode resonators (CMRs) have been widely investigated [13–15]. The CMRs have the advantages of photolithographic defined high operating frequencies compared to other techniques. However, there are several loss mechanisms in CMRs, such as interface loss from the connection of electrodes and AlN thin film, damping loss from the resonators and anchor loss, which limit the applications of AlN-based CMRs [16–20]. A large amount of energies leak through the anchor to the piezoelectric plate in the AlN resonators, i.e. the anchor loss [21–25]. Zou and Chih-Ming *et al.* [26] have designed the beveled and rounded butterfly-

shaped AlN CMRs. Acoustic wave reflectors are formed at the transition areas between the anchor and vibration region, such design enables to push waves away from the anchors, so the energy is suppressed. Yung-Yu Chen *et al.* [16] have investigated the AlN CMRs convex free edges to reduce the anchor loss and then improve Q factor. In our work, another efficient way to reduce the anchor loss of the AlN-based CMRs is demonstrated utilizing half circle shaped reflectors to push acoustic waves back to the resonate region.

To decrease the energy leakage from anchor loss, we demonstrate an AlN CMR with half circle shaped reflectors. Fig. 1(a) illustrates a normal AlN CMR employing the normal plate. As shown in Fig. 1(b), The AlN CMR with half circle shaped reflector is utilized to reduce the anchor loss in AlN CMRs. Unlike the AlN CMRs with normal plate, the CMRs with half circle shaped reflectors can limit the propagation of acoustic wave to the substrate plate. We utilize the COMSOL Multiphysics[®] to show the improvement on the Q factor of the CMRs. In addition, AlN CMRs with half circle shaped reflectors are experimentally fabricated, and present a higher Q factor compared to the CMRs with a normal plate configuration.

II. DESIGN AND SIMULATION

The main energy dissipation mechanisms for piezoelectric resonators can be expressed as [16],

$$\frac{1}{Q} = \frac{1}{Q_{interface}} + \frac{1}{Q_{anchor\ loss}} + \frac{1}{Q_{other}} \quad (1)$$

In order to investigate the influence of anchor loss in the AlN CMRs, we assume that the main vibration energy dissipation in the CMRs is anchor loss, and $Q_{anchor\ loss}$ is mainly contributes to the Q of AlN CMRs. Anchor loss is determined by the displacement fields in the anchor and plate. Our design aims to decrease the displacement fields in the plate to reduce anchor loss, and then increase the total Q factor of the AlN CMRs, the geometric dimensions of AlN CMRs are listed in the Table 1. In the AlN CMRs with

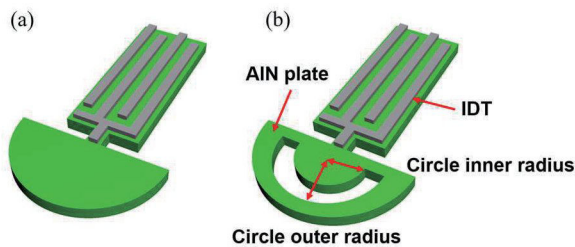


Fig. 1 Illustrations of AlN CMRs with (a) normal plate, (b) half circle shaped reflector.

Table 1 Geometric dimensions of AlN CMRs

Parameters	Normal	Half circle shaped
IDT numbers	4	4
IDT aperture	180 μm	180 μm
IDT coverage	0.5	0.5
Anchor length	4.9 μm	4.9 μm
Anchor width	8.2 μm	8.2 μm
Wavelength	20 μm	20 μm
Circle inner radius	NA	17.5 μm
Circle outer radius	NA	27.5 μm

¹School of Information Science and Technology, ShanghaiTech University

²Shanghai Institute of Microsystem and Information Technology, Chinese Academy of Sciences

³University of Chinese Academy of Sciences

*Corresponding Authors:

Zhifang, Luo, (e-mail: luozhf@shanghaitech.edu.cn),

Tao Wu, (e-mail: wutao@shanghaitech.edu.cn),

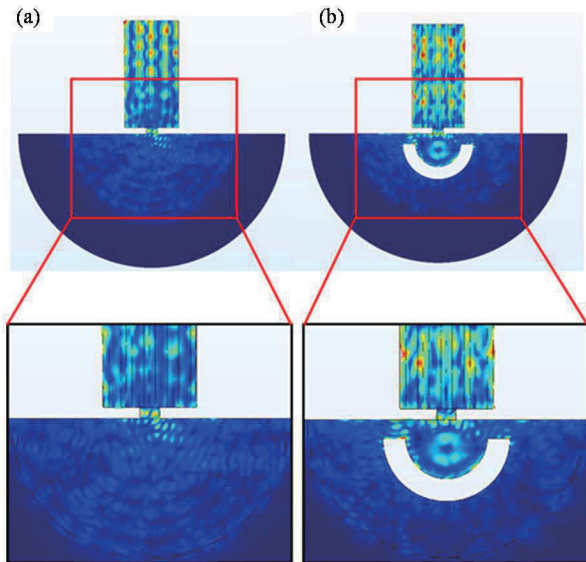


Fig. 2 Simulated displacement fields of AIN CMRs with (a) normal plate, (b) half circle shaped reflector.

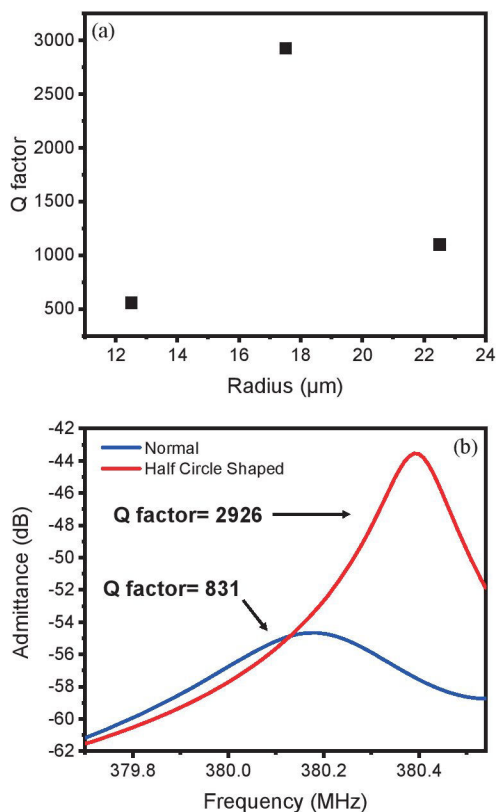


Fig. 3 (a) Simulated Q factor of AIN CMRs with different inner circle radius. (b) Simulated admittance response of AIN CMRs with normal plate and half circle shaped reflector.

normal plate, the acoustic wave in the vibration region would propagate through anchor to the substrate plate, resulting large anchor loss. By using the half circle shaped reflectors, the acoustic wave reflector can reflect acoustic wave effectively to the active region.

Perfectly matched layer (PML)-based finite element analysis from COMSOL Multiphysics[®] software are used to investigate the displacement fields on the vibration region and plate [16, 17, 26]. The AIN CMRs with anchors are attached to the semi-cylinder plates and then covered by the PMLs, the radius of semi-cylinder plates is set as three times wavelength, and the radius of PMLs are set as five times wavelength, which aims to absorb the acoustic wave efficiently. The design of anchor width and length is also essential to reduce anchor loss. Yung-Yu Chen *et al.* [16], B P Harrington and R Abdolvand [17] have investigated the influence of different designs, so our anchor length and width are designed based on their findings. Fig. 2 presents the displacement fields of AIN CMRs with the normal plate and half circle shaped reflectors at S0 mode utilizing FEA simulation. Brighter color means larger displacement fields. $V_{\text{RF}} = 1 \text{ V}$ is applied to the IDT to induce S0 mode of AIN CMRs. To reduce memory of computation, only half of the CMR and plate are simulated. As illustrated in Fig. 2(a), there is large displacement in the piezoelectric thin film of the normal design, which means a lot of energies leaked from piezoelectric layer, resulting in the big anchor loss of the AIN CMRs. In addition, as a lot of energy loss in plate via anchor, the displacement fields near the anchor in AIN CMRs is reduced dramatically by energy dissipation. Fig. 2(b) shows that the displacement fields away from the anchor are similar with those of normal design, but the displacement fields in the piezoelectric plate are obviously less than those in the normal plate. Since a large amount of energies are reflected back to the CMRs by half circle shaped reflectors, only small part is absorbed by PMLs. It makes much larger displacement fields in the vibration region near the anchor. As seen in Fig. 3(a), the best performance for simulated resonators is found for inner circle radius of $17.5 \mu\text{m}$. Fig. 3(b) illustrates the admittance response of AIN CMRs with and without half circle shaped reflectors. The admittance response is simulated in the 3D frequency domain analysis by a frequency spacing of 10 kHz . The simulated Q of S0 mode in the AIN CMR with half circle shaped reflectors is 2926, while the Q of the AIN CMR with normal plate is only 831. The simulated Q is increased by 252 %.

III. FABRICATION AND CHARACTERIZATION

In order to validate the results of the simulation results, AIN CMRs with normal plates and half circle shaped reflectors are fabricated on the same wafer.

For the sample preparation, $1 \mu\text{m}$ (0002) polar AIN is deposited on high-resistive silicon wafer at 300°C by reactive magnetron sputtering system with a 12 inch Al target. Fig. 4(a) illustrates the surface morphology of AIN thin film by scanning electron microscopy Carl Zeiss Gemini300. AIN grains are uniformly and densely aligned, which indicates the great crystal quality of the sputtered thin films. It can be seen from Fig. 4(b) that the AIN thin film is well deposited on the silicon wafer with great c-axis oriented crystal columns. As shown in Fig. 4(c), the roughness of AIN surface is measured by Atomic Force Microscopy from Asylum Research, and the value of RMS is only 970 pm , which shows great surface uniformity of AIN piezoelectric thin film. Such uniform and great z-axis oriented AIN thin film is necessary to fabricate devices based on it, which enables less energy dissipation in the piezoelectric thin film,

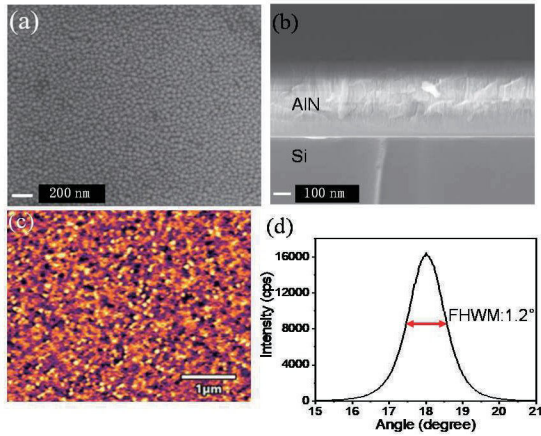


Fig. 4 SEM images of (a) (0002) polar AIN surface, (b) (0002) polar AIN crosssection view, (c) AFM height image of (0002) polar AIN surface, (d) XRD rocking curve of AIN thin film.

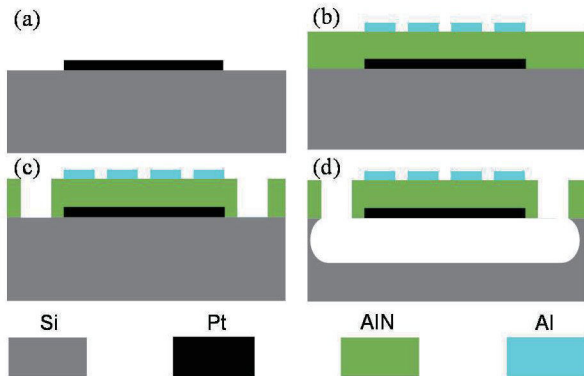


Fig. 5 (a) Lift-off Ti/Pt layer as bottom electrode, (b) deposit AIN thin film and pattern Al as top electrode, (c) ICP dry etching, (d) release AIN CMRs via XeF_2 .

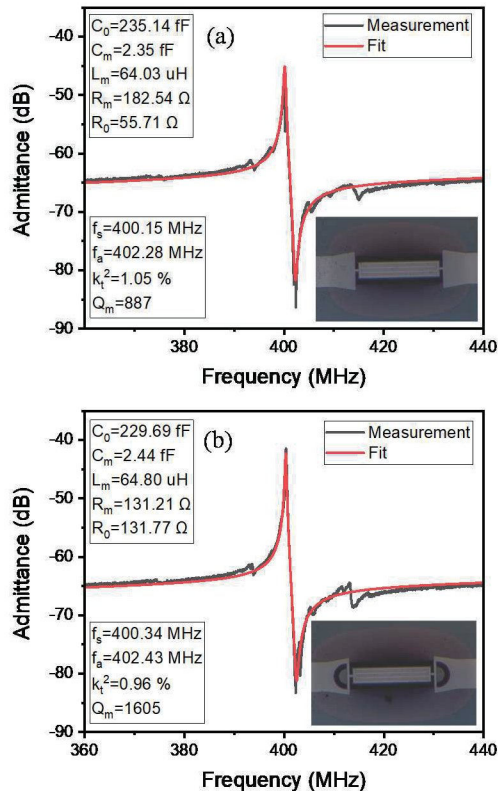


Fig. 6 The admittance response of AIN CMRs with (a) normal plate, and (b) half circle shaped reflector.

resulting in higher performance devices. The crystal orientation of AIN is measured by X-ray diffraction (XRD) by PANalytical[®] Empyrean system, the full width at half maximum (FWHM) of AIN thin film is 1.2° , as illustrated in Fig. 4(d).

The fabrication of AIN CMRs is a traditional 4-mask process on high-resistive (100) silicon wafer, as seen in Fig. 5 (a)-(d). First, the physical vapor deposition (PVD) is utilized to deposit and pattern 10 nm Ti/ 100 nm Pt via a lift-off process as bottom electrode. Then, 1 μm AIN piezoelectric thin film is deposited utilizing EVATEC CLN200 reactive magnetron sputtering system. Then, a 200 nm Al layer is deposited and patterned to define the top interdigitated electrodes (IDT). Next, the ICP etching is used to define the active region of AIN CMRs as well as the half circle shaped reflectors. Finally, the CMRs are released by XeF_2 . To reduce the fabrication process variations, all the AIN CMRs we discussed here are fabricated on the same wafer and placed in the vicinity.

According to our FEA simulation and analysis, the quality factor Q of AIN CMR with half circle shaped reflectors is significantly higher than the AIN CMR with normal plate. The fabricated AIN CMRs are characterized by Keysight[®] N5234B PNA-L Network Analyzer. The measured Q of CMRs are extracted from the admittance response by dividing the resonance frequencies by the -3 dB bandwidth. Fig. 6(a) and Fig. 6(b) present the one-port admittance response for the AIN CMRs based on normal plate and half circle shaped reflectors, respectively. The AIN CMR with half circle shaped reflectors yields a Q factor of 1605, upwards 80 % over a normal AIN CMR which has a Q of 887, which shows higher Q improvement compared to the previous works. Zou and Chih-Ming *et al.* [26] present 67 % improvement of measured Q , Chih-Ming *et al.* [18] indicate 50 % measured Q improvement to the normal design. In the FEA simulation, loss of the resonator is set larger than the actual situation, so that the measured Q is a little larger than the simulated Q in the CMRs with normal plate. Due to the loss of the manufacturing process, the measured Q of CMRs with half circle shaped reflectors is lower than the simulated value. The electrical response of piezoelectric resonators is usually represented with the modified Butterworth-Van Dyke (mBVD) model [27]. After fitting into the mBVD model, the C_0 , C_m , L_m , R_m , R_0 are all extracted, where C_0 and R_0 are the static capacitance and static resistance of resonators, respectively. C_m , L_m , R_m are the motional capacitance, motional inductance, motional resistance of resonators, respectively.

IV. CONCLUSION

A design of AIN CMR with half circle shaped reflectors is presented in this work. PML-based FEA simulation confirms the influence of half circle shaped reflectors on the reduction of displacement fields in the piezoelectric plate and resonate region near the anchor and improvement of Q . Such reflector can efficiently reflect the acoustic wave back to the resonator, significantly reduce the energy loss. The AIN CMR with half circle shaped reflectors yields a Q of 1605, showing 80% increase in Q over AIN CMR with normal plate.

V. ACKNOWLEDGMENTS

The authors appreciate the support from the ShanghaiTech Quantum Device Lab (SQDL), and Analytical Instrumentation Center (SPSTAIC10112914) XRD Lab, Natural Science Foundation of Shanghai (19ZR1477000) and National Natural Science Foundation of China (61874073).

REFERENCES

- [1] A. Gao, K. Liu, J. Liang, T. Wu, "AlN MEMS filters with extremely high bandwidth widening capability," *Microsyst. Nanoeng.*, vol. 6, no. 1, p. 74, Dec. 2020.
- [2] C. Caliendo, P. Imperatori, "High-frequency, high-sensitivity acoustic sensor implemented on ALN/Si substrate," *Appl. Phys. Lett.*, vol. 83, no. 8, pp. 1641–1643, Aug. 2003.
- [3] V. Yantchev, I. Katardjiev, "Thin film Lamb wave resonators in frequency control and sensing applications: a review," *J. Micromechanics Microengineering*, vol. 23, no. 4, p. 043001, 2013.
- [4] L. Wang, B. Wu, J. Chen, H. Liu, P. Hu, Y. Liu, "Monolayer hexagonal boron nitride films with large domain size and clean interface for enhancing the mobility of graphene-based field-effect transistors," *Adv. Mater.*, vol. 26, no. 10, pp. 1559–1564, 2014.
- [5] Q.-X. Su, P. Kirby, E. Komuro, M. Imura, Q. Zhang, R. Whatmore, "Thin-film bulk acoustic resonators and filters using ZnO and lead-zirconium-titanate thin films," *IEEE Trans. Microw. Theory Tech.*, vol. 49, no. 4, pp. 769–778, Apr. 2001.
- [6] J. L. Hockel, T. Wu, G. P. Carman, "Voltage bias influence on the converse magnetoelectric effect of PZT/terfenol-D/PZT laminates," *J. Appl. Phys.*, vol. 109, no. 6, Art. no. 6, 2011.
- [7] M.-H. Li, C.-Y. Chen, R. Lu, Y. Yang, T. Wu, S. Gong, "Power-Efficient Ovenized Lithium Niobate SHO Resonator Arrays with Passive Temperature Compensation," in *2019 IEEE 32nd International Conference on Micro Electro Mechanical Systems (MEMS)*, Seoul, Korea (South), Jan. 2019, pp. 911–914.
- [8] M.-A. Dubois, P. Muralt, "Properties of aluminum nitride thin films for piezoelectric transducers and microwave filter applications," *Appl. Phys. Lett.*, vol. 74, no. 20, Art. no. 20, 1999.
- [9] T. Wu, G. Chen, C. Cassella, W. Z. Zhu, M. Assylbekova, M. Rinaldi, N. McGruer, "Design and fabrication of AlN RF MEMS switch for near-zero power RF wake-up receivers," in *2017 IEEE SENSORS*, Glasgow, Oct. 2017, pp. 1–3.
- [10] Z. Luo, S. Shao, T. Wu, "Characterization of ALN and ALSCN film ICP etching for micro/nano fabrication," *Microelectron. Eng.*, p. 111530, Feb. 2021.
- [11] T. Wu, Z. Qian, M. Rinaldi, "Low cost thin film encapsulation for AlN resonators," in *2018 IEEE Micro Electro Mechanical Systems (MEMS)*, Belfast, Jan. 2018, pp. 1024–1027.
- [12] J. Zou, A. Gao, A. P. Pisano, "Spectrum-clean S₁ AlN Lamb wave resonator with damped edge reflectors," *Appl. Phys. Lett.*, vol. 116, no. 2, p. 023505, Jan. 2020.
- [13] G. Wingqvist, "AlN-based sputter-deposited shear mode thin film bulk acoustic resonator (FBAR) for biosensor applications — A review," *Surf. Coat. Technol.*, vol. 205, no. 5, pp. 1279–1286, Nov. 2010.
- [14] J. G. Rodriguez-Madrid, G. F. Iriarte, J. Pedros, O. A. Williams, D. Brink, F. Calle, "Super-High-Frequency SAW Resonators on AlN/Diamond," *IEEE Electron Device Lett.*, vol. 33, no. 4, pp. 495–497, Apr. 2012.
- [15] M. Giovannini, S. Yazici, N.-K. Kuo, G. Piazza, "Apodization technique for spurious mode suppression in AlN contour-mode resonators," *Sens. Actuators Phys.*, vol. 206, pp. 42–50, Feb. 2014.
- [16] Y.-Y. Chen, Y.-T. Lai, C.-M. Lin, "Finite element analysis of anchor loss in AlN Lamb wave resonators," in *2014 IEEE International Frequency Control Symposium (FCS)*, Taipei, Taiwan, May 2014, pp. 1–5.
- [17] B. P. Harrington, R. Abdolvand, "In-plane acoustic reflectors for reducing effective anchor loss in lateral-extensional MEMS resonators," *J. Micromechanics Microengineering*, vol. 21, no. 8, p. 085021, Jul. 2011.
- [18] C. Lin, J. Hsu, D. G. Senesky, A. P. Pisano, "Anchor loss reduction in ALN Lamb wave resonators using phononic crystal strip tethers," in *2014 IEEE International Frequency Control Symposium (FCS)*, May 2014, pp. 1–5.
- [19] J. Segovia-Fernandez, M. Cremonesi, C. Cassella, A. Frangi, G. Piazza, "Anchor Losses in AlN Contour Mode Resonators," *J. Microelectromechanical Syst.*, vol. 24, no. 2, pp. 265–275, Apr. 2015.
- [20] J. Zou, C.-M. Lin, A. P. Pisano, "Anchor loss suppression using butterfly-shaped plates for AlN Lamb wave resonators," in *2015 Joint Conference of the IEEE International Frequency Control Symposium & the European Frequency and Time Forum*, 2015, pp. 432–435.
- [21] C.-M. Lin, Y.-J. Lai, J.-C. Hsu, Y.-Y. Chen, D. G. Senesky, A. P. Pisano, "High-Q aluminum nitride Lamb wave resonators with biconvex edges," *Appl. Phys. Lett.*, vol. 99, no. 14, p. 143501, 2011.
- [22] C. Cassella, N. Singh, B. W. Soon, G. Piazza, "Quality factor dependence on the inactive regions in AlN contour-mode resonators," *J. Microelectromechanical Syst.*, vol. 24, no. 5, pp. 1575–1582, 2015.
- [23] B. Gibson, K. Qalandar, C. Cassella, G. Piazza, K. L. Foster, "A study on the effects of release area on the quality factor of contour-mode resonators by laser doppler vibrometry," *IEEE Trans. Ultrason. Ferroelectr. Freq. Control*, vol. 64, no. 5, pp. 898–904, 2017.
- [24] C. Tu, J. E.-Y. Lee, "VHF-band biconvex AlN-on-silicon micromechanical resonators with enhanced quality factor and suppressed spurious modes," *J. Micromechanics Microengineering*, vol. 26, no. 6, p. 065012, Jun. 2016.
- [25] C. Tu, J. E.-Y. Lee, "A semi-analytical modeling approach for laterally-vibrating thin-film piezoelectric-on-silicon micromechanical resonators," *J. Micromechanics Microengineering*, vol. 25, no. 11, p. 115020, Nov. 2015.
- [26] J. Zou, C. Lin, G. Tang, A. P. Pisano, "High-Q Butterfly-Shaped AlN Lamb Wave Resonators," *IEEE Electron Device Lett.*, vol. 38, no. 12, pp. 1739–1742, Dec. 2017.
- [27] J. D. Larson, P. D. Bradley, S. Wartenberg, R. C. Ruby, "Modified Butterworth-Van Dyke circuit for FBAR resonators and automated measurement system," in *2000 IEEE Ultrasonics Symposium. Proceedings. An International Symposium*, 2000, vol. 1, pp. 863–868.